

## Imaging

# Assessment of myocardial ischaemia and viability: role of positron emission tomography

Nina Ghosh<sup>1</sup>, Ornella E. Rimoldi<sup>2,3</sup>, Rob S.B. Beanlands<sup>1</sup>, and Paolo G. Camici<sup>3,4\*</sup>

<sup>1</sup>National Cardiac PET Centre, Division of Cardiology and the Molecular Function and Imaging Program, University of Ottawa Heart Institute, Ottawa, ONT, Canada; <sup>2</sup>CNR Clinical Physiology Institute, Pisa, Italy; <sup>3</sup>National Heart and Lung Institute, Imperial College, London, UK; and <sup>4</sup>Vita-Salute University and Scientific Institute San Raffaele Milan, Via Olgettina 60, 20132 Milan, Italy

Received 13 July 2010; revised 13 August 2010; accepted 25 August 2010; online publish-ahead-of-print 21 October 2010

In developed countries, coronary artery disease (CAD) continues to be a major cause of death and disability. Over the past two decades, positron emission tomography (PET) imaging has become more widely accessible for the management of ischemic heart disease. Positron emission tomography has also emerged as an important alternative perfusion imaging modality in the context of recent shortages of molybdenum-99/technetium-99m (<sup>99m</sup>Tc). The clinical application of PET in ischaemic heart disease falls into two main categories: first, it is a well-established modality for evaluation of myocardial blood flow (MBF); second, it enables assessment of myocardial metabolism and viability in patients with ischaemic left ventricular dysfunction. The combined study of MBF and metabolism by PET has led to a better understanding of the pathophysiology of ischaemic heart disease. While there are potential future applications of PET for plaque and molecular imaging, as well as some clinical use in inflammatory conditions, this article provides an overview of the physical and biological principles behind PET imaging and its main clinical applications in cardiology, namely the assessment of MBF and metabolism.

**Keywords** Myocardial ischaemia • PET

## Introduction

In developed countries, coronary artery disease (CAD) continues to be a major cause of death and disability.<sup>1</sup> Over the past two decades, positron emission tomography (PET) imaging has become more widely accessible for the management of ischaemic heart disease. Positron emission tomography has also emerged as an important alternative perfusion imaging modality in the context of recent shortages of molybdenum-99/technetium-99m (<sup>99m</sup>Tc).<sup>2</sup> The clinical application of PET in ischaemic heart disease falls into two main categories: first, it is a well-established modality for evaluation of myocardial blood flow (MBF); second, it enables assessment of myocardial metabolism and viability in patients with ischaemic left ventricular (LV) dysfunction. The combined study of MBF and metabolism by PET has led to a better understanding of the pathophysiology of ischaemic heart disease.<sup>3</sup> While there are potential future applications of PET for plaque and molecular imaging, as well as some clinical use in inflammatory conditions, this article provides an overview of the physical and biological principles behind PET imaging and its main clinical applications in cardiology, namely the assessment of MBF and metabolism.

## Myocardial perfusion imaging and quantification of flow

### Available positron emission tomography tracers

Radiotracers are molecules that closely resemble naturally occurring molecules rendering them useful for characterizing physiologically relevant processes in qualitative and quantitative terms.<sup>4</sup> Cardiac PET radiotracers can be classified into those that enable assessment of (i) myocardial perfusion and (ii) myocardial metabolism.<sup>5</sup> (see section on assessment of myocardial metabolism and *Figure 1*)

### Positron emission tomography perfusion radiotracers

*Rubidium-82* (<sup>82</sup>Rb) is a cation with properties similar to potassium and thus its myocardial uptake involves Na<sup>+</sup>/K<sup>+</sup> ATPase-dependent mechanisms. It has a half-life of 76 s and a first-pass extraction fraction of 65%. Because myocardial extraction of <sup>82</sup>Rb at higher flow rates is diminished, the uptake/flow relationship

\* Corresponding author. Tel: +39 226 436 202, Fax: +39 226 436 218, Email [camici.paolo@hsr.it](mailto:camici.paolo@hsr.it)

Published on behalf of the European Society of Cardiology. All rights reserved. © The Author 2010. For permissions please email: [journals.permissions@oxfordjournals.org](mailto:journals.permissions@oxfordjournals.org)

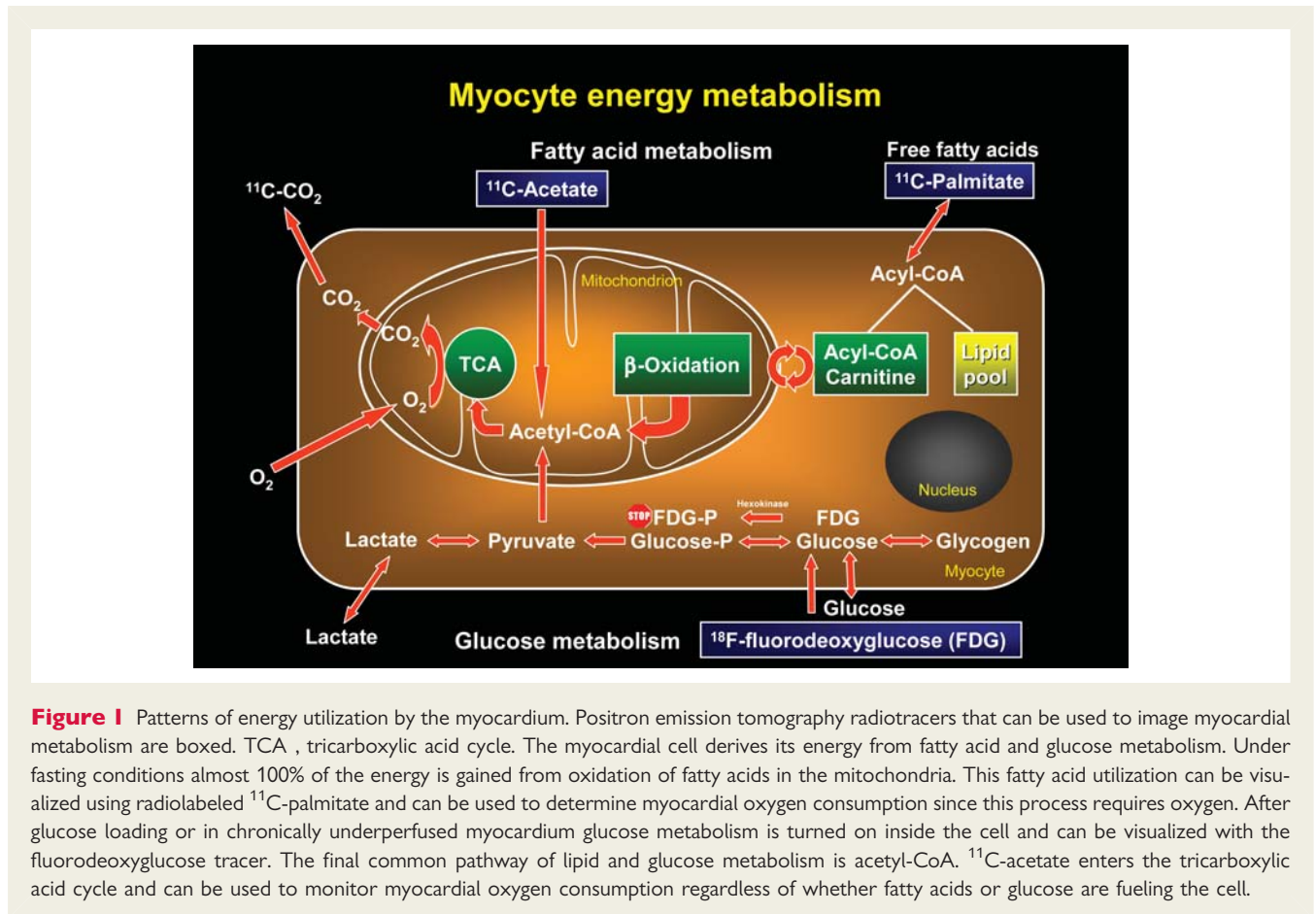


**Figure 1** Patterns of energy utilization by the myocardium. Positron emission tomography radiotracers that can be used to image myocardial metabolism are boxed. TCA, tricarboxylic acid cycle. The myocardial cell derives its energy from fatty acid and glucose metabolism. Under fasting conditions almost 100% of the energy is gained from oxidation of fatty acids in the mitochondria. This fatty acid utilization can be visualized using radiolabeled <sup>11</sup>C-palmitate and can be used to determine myocardial oxygen consumption since this process requires oxygen. After glucose loading or in chronically underperfused myocardium glucose metabolism is turned on inside the cell and can be visualized with the fluorodeoxyglucose tracer. The final common pathway of lipid and glucose metabolism is acetyl-CoA. <sup>11</sup>C-acetate enters the tricarboxylic acid cycle and can be used to monitor myocardial oxygen consumption regardless of whether fatty acids or glucose are fueling the cell.

becomes non-linear as flow increases. Unlike nitrogen-13 ammonia (<sup>13</sup>NH<sub>3</sub>) and oxygen-15 labeled water (H<sub>2</sub><sup>15</sup>O), which require cyclotrons onsite, <sup>82</sup>Rb is produced by a Strontium-82/<sup>82</sup>Rb generator that generally requires replacement once a month.<sup>6</sup>

*N-13 Ammonia* is an extractable perfusion tracer whose transmembrane transport occurs by passive diffusion or by the active Na<sup>+</sup>/K<sup>+</sup>ATPase mechanism. Myocyte retention of <sup>13</sup>NH<sub>3</sub> is energy requiring and involves metabolic trapping.<sup>7</sup> It has an 80% first-pass extraction fraction and a half-life of 10 min.<sup>6</sup> Good quality images can be obtained using <sup>13</sup>NH<sub>3</sub> because of its high myocardial retention; its rapid clearance from the blood pool and the positron range of <sup>13</sup>N. Furthermore, MBF measured using <sup>13</sup>NH<sub>3</sub> can be quantified over a broad range of flow rates.<sup>8</sup> At higher flow rates, flow can be somewhat underestimated using <sup>13</sup>NH<sub>3</sub>, but to a lesser extent than with <sup>82</sup>Rb.

*O-15 water* (H<sub>2</sub><sup>15</sup>O) is a freely diffusible perfusion tracer with a virtually 100% first-pass extraction.<sup>9</sup> This tracer is not trapped in the myocardium, but rather reaches equilibrium between extra- and intravascular compartments making it difficult to obtain clear perfusion images with H<sub>2</sub><sup>15</sup>O in contrast to <sup>13</sup>NH<sub>3</sub> and <sup>82</sup>Rb. Oxygen-15 labeled water has a half-life of 2 min and is recognized to be the most suitable tracer for non-invasive measurement of MBF.<sup>10</sup> However, the application of H<sub>2</sub><sup>15</sup>O perfusion imaging, so far, has been primarily investigational.<sup>3,11</sup>

## Image acquisition and interpretation

Positron emission tomography imaging uses scanners that are optimized to detect positron-emitting radioisotopes.<sup>12</sup> Radioactive decay of a nucleus causes it to emit a positively charged particle called a positron ( $\beta^+$ ). After a few millimetres of travel in the tissue, the positron collides with an electron resulting in annihilation of both particles and release of energy in the form of two high-energy photons. The two 511 keV photons travel exactly 180° from each other.<sup>6</sup> Positron emission tomography detectors are programmed to detect events with temporal coincidence of photons that strike at directly opposing detectors. Coincidence photon detection enables count sensitivity without the need for collimation. This represents an important advantage over single photon emission computed tomography (SPECT) imaging. The spatial resolution of current PET scanners is in the range of 4–7 mm. Positron emission tomography imaging incorporates algorithms that correct for photon attenuation and scatter. Attenuation correction can be accurately and reliably achieved with PET either using radioactive sources or using CT on hybrid scanners. One advantage of transmission CT-based attenuation correction is the fast acquisition (<1 min).<sup>13</sup> New methods to obtain quantitative MBF imaging without the need for attenuation correction are currently under study.<sup>14</sup>

Full details of image acquisition are beyond the scope of this article. The reader is referred to American Society of Nuclear

Cardiology (ASNC) guidelines<sup>15</sup> for cardiac PET for recommended image acquisition protocols.

## Assessment of ischaemia and early disease detection with perfusion and flow quantification

### Perfusion imaging

In the past few years, there has been a significant increase in the dissemination of PET instrumentation for the performance of myocardial perfusion imaging (MPI).<sup>16</sup> Important components of PET MPI protocols include: (i) *patient preparation*: including fasting and abstinence from caffeine and theophylline-containing medications; (ii) *scout scanning*: to ensure correct patient positioning; (iii) *transmission scans*: before rest and after stress for attenuation correction; and (iv) *emission scans*: when radioactivity is detected from the patient, done at rest and stress. Details pertaining to common protocols used for imaging myocardial perfusion with dedicated PET or PET/CT can be found elsewhere.<sup>15,17</sup> Visual comparison of stress and rest images may reveal: (i) *normal myocardium* that shows uniform radiotracer uptake at stress and rest; (ii) *the presence of ischaemic myocardium* in which a perfusion defect is seen on stress, but not rest images; a so-called 'reversible defect' (Figure 2); (3) *the presence of scar* in which perfusion defects are seen both at stress and rest; a so-called 'fixed defect'. Some fixed defects may also contain hibernating (i.e. dysfunctional but viable) myocardium and additional viability methods such as <sup>18</sup>F-fluorodeoxyglucose (<sup>18</sup>FDG). Positron emission tomography imaging is required to rule out hibernation. The additional information provided by *flow quantification* is outlined in more detail in the subsequent section.

Compared to most SPECT perfusion tracers, PET perfusion tracers used in clinical practice have more linear uptake-flow relationships even at higher flow rates (>2.5 mL/min/g).<sup>17</sup> Although attenuation effects are significantly greater with PET compared with SPECT due to coincidence photons and full-ring acquisition, algorithms to correct for attenuation are more accurate with PET.<sup>18</sup> Furthermore, both better spatial resolution and contrast resolution (target-to-background ratio) in PET enable enhanced detection of milder perfusion abnormalities with PET in comparison with SPECT. The short physical half-life of commonly used PET tracers, enables a short acquisition time enhancing patient comfort and decreased potential for patient motion, but makes exercise imaging difficult. Thus, PET MPI is predominantly performed under pharmacological stress.<sup>17</sup>

Several studies have confirmed the diagnostic advantage of PET MPI over conventional SPECT MPI.<sup>19,20</sup> Most recently, <sup>82</sup>Rb PET MPI was compared with contemporary <sup>99m</sup>Tc-sestamibi SPECT.<sup>16</sup> Not only PET perfusion images were significantly better in quality than SPECT, but also significantly more accurate (93% vs. 73%) for identifying significant CAD (stenoses  $\geq 50\%$ ). However, the results of this study should be interpreted with caution as this was not a head-to-head comparison, but rather, PET and SPECT populations were propensity matched for characteristics known to impact perfusion data. Overall, these studies indicate that for patients who require pharmacologic stress, PET imaging provides superior diagnostic accuracy and may be preferable in situations in which SPECT image quality is expected to be degraded by soft-tissue attenuation (such as in obese patients) or when it is important to determine the functional significance of a known coronary lesion.

The prognostic value of PET MPI has also been demonstrated in several studies.<sup>21–23</sup> Yoshinaga et al.<sup>22</sup> showed that events rates

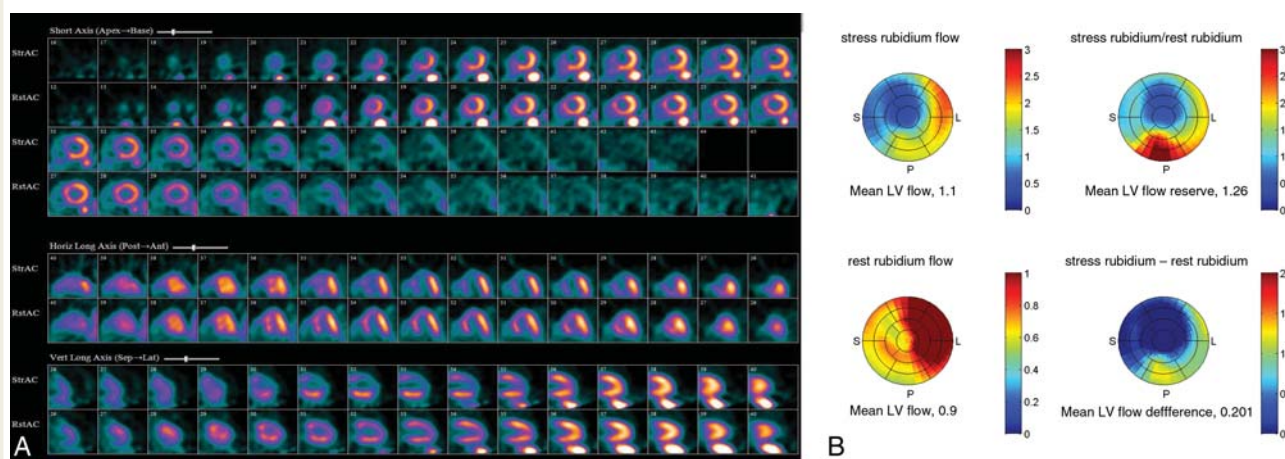


**Figure 2** Rubidium-82 stress myocardial perfusion scan and flow quantification. Dipyridamole <sup>82</sup>Rb positron emission tomography scan showing severe reduction in uptake in the anteroseptal region at stress with significant improvement in uptake at rest indicating significant myocardial ischaemia in the left anterior descending artery (LAD) territory (A). Absolute flow quantification showing an increase in mean LV blood flow from 0.9 at rest to only 1.1 at stress, corresponding to a coronary flow reserve of only 1.26. (B). Subsequent cardiac catheterization showed a 90% lesion in the proximal LAD (image not shown). StrAC, stress acquisition; RstAC, rest acquisition; LV, left ventricle.

increased with increasing summed stress score (SSS) and that  $^{82}\text{Rb}$  PET SSS was the strongest predictor of total cardiac events. Likewise, Marwick *et al.*<sup>21</sup> demonstrated that PET MPI provided incremental prognostic value over clinical and angiographic findings alone. Dorbala *et al.*<sup>23</sup> showed that LV ejection fraction (EF) reserve (stress minus rest LVEF) obtained from gated PET images, provides significant independent and incremental value for predicting future adverse events and Lertsburapa *et al.*<sup>24</sup> showed that decreased stress EF and increased SSS had prognostic value for prediction of all-cause mortality.

Thus, PET MPI has high diagnostic accuracy and good prognostic value in patients being assessed for CAD and ischaemia.

## Flow quantification

Accurate absolute quantification of MBF enables the calculation of coronary flow reserve (CFR), the ratio of peak MBF during near maximal pharmacologically induced vasodilatation to resting MBF. Coronary flow reserve is an index of the functional significance of a coronary stenosis.<sup>25</sup> In patients with CAD, CFR decreases in proportion to the degree of stenosis severity and is exhausted (i.e. hyperaemic MBF = resting MBF) for stenoses  $\geq 80\%$  of the luminal diameter.<sup>25,26</sup> In severe stenosis, regardless of the MBF level under resting conditions any increase of cardiac workload and oxygen demand cannot be met by an adequate increase in MBF, thus leading to demand ischaemia. With quantitative MBF measurement, it is possible to challenge the function of the coronary microcirculation by measuring CFR. Positron emission tomography is particularly effective in circumstances where CFR is diffusely blunted, for example in patients with hypertrophic cardiomyopathy, aortic stenosis, hypertensive heart disease where, in the absence of epicardial disease,<sup>27–29</sup> the reduced CFR is due to coronary microvascular dysfunction.<sup>3</sup> Measurement of CFR enables the differentiation of pathological from physiologic LV hypertrophy<sup>30</sup> as well as the exclusion of myocardial ischaemia in patients with chest pain and angiographically normal coronary arteries.<sup>31</sup> Some caution should be taken when interpreting CFR values in the elderly. There is a linear association between age and resting MBF partially related to changes in external cardiac workload and hyperaemic MBF, which declines over 55 years of age.<sup>32</sup>

Recently two studies have demonstrated the prognostic value of flow quantification in patients with CAD. Tio *et al.*<sup>33</sup> showed that patients with LV dysfunction and CFR  $< 1.49$  on  $^{13}\text{NH}_3$  MBF quantification had worse survival. Likewise Herzog *et al.*<sup>34</sup> using  $^{13}\text{NH}_3$  MBF quantification, showed that in patients with normal relative perfusion, preserved CFR ( $> 2.0$ ) had a good prognosis for at least a 3 year period compared with patients with reduced CFR. The authors suggest that this may be due to detection of early atherosclerotic microvascular disease. These authors also demonstrated that when a relative perfusion defect was present, reduced CFR was linked to worse cardiac outcomes (major adverse cardiac events and cardiac death) at a mean follow-up of 5.5 years (Figure 3).<sup>34</sup> Recent preliminary data indicate that flow quantification using  $^{82}\text{Rb}$  is sensitive for detection of multi-vessel disease and may also have prognostic value on 1 year follow-up.<sup>35,36</sup>

*F-18-fluorobenzyl triphenyl phosphonium* and  $^{18}\text{F}$ -flupiridaz (BMS-747158–02) are new PET perfusion imaging agents. These tracers bind to the mitochondrial complex I of the electron transport chain with high affinity. They demonstrate good uptake in the heart due to its high density of mitochondria.  $^{18}\text{F}$ -flupiridaz is about to enter Phase 3 studies. Early reports note good quality imaging and several promising features. A relatively long half-life provides good contrast between the heart and surrounding tissues that remains stable over time. Its high extraction at first pass is not affected by high flow rates. The half-life of 110 min could enable exercise PET imaging. Flow quantification may also be possible with these new agents.<sup>37–39</sup> Finally, it does not require an on-site cyclotron.

## Assessment of myocardial metabolism and viability using positron emission tomography

### Metabolism in normal and ischaemic myocardium

Patterns of substrate uptake and utilization by the human myocardium show marked oscillation between the fasting state, with low rates of uptake of glucose and lactate and the high rates of uptake and oxidation of free fatty acid (FFA), and the fed state with high rates of uptake and oxidation of glucose and lactate and low FFA uptake. Glycolysis is the metabolic pathway converting glucose 6-phosphate to pyruvate. The basic control mechanisms operative during myocardial ischaemia are increased glycogen breakdown and increased glucose uptake; both feed products into the pathways of glycolysis, which are accelerated by anaerobiosis (Pasteur effect). Eventually, however, the products of anaerobic glycolysis, namely protons, NADH<sub>2</sub>, and lactate can feed back to inhibit glycolysis at various levels.

Non-invasive metabolic imaging of ischaemia basically relies on two simple observations. First, the uptake of glucose by the myocardium is increased by hypoxia and mild-to-moderate ischaemia, but decreased by very severe ischaemia. Second, during both mild and severe ischaemia the extraction, uptake, and oxidation of FFA are reduced. Hence, the uptake of an appropriately labelled FFA is seen to be decreased in the ischaemic myocardium.

### Ischaemia: stunning, repetitive stunning and hibernation

Ischaemia results when supply of nutrient flow cannot meet the demand of the tissue. Over 75 years ago Tennant and Wiggers<sup>40</sup> demonstrated that acute ischaemia rapidly impairs myocardial contractile function. Forty years later, Heyndrickx *et al.*<sup>41</sup> showed that this dysfunction persisted for several hours after transient non-lethal ischaemia, but eventually resulted in full functional recovery. This phenomenon known as *myocardial stunning*<sup>42</sup> has been demonstrated to occur in patients with CAD.<sup>43,44</sup>

Diamond *et al.*<sup>45</sup> were the first to use the term *myocardial hibernation*. Rahimtoola<sup>46</sup> expanded and increased the awareness of this concept, hypothesizing that chronic myocardial ischaemia could cause chronic, but reversible myocardial dysfunction.

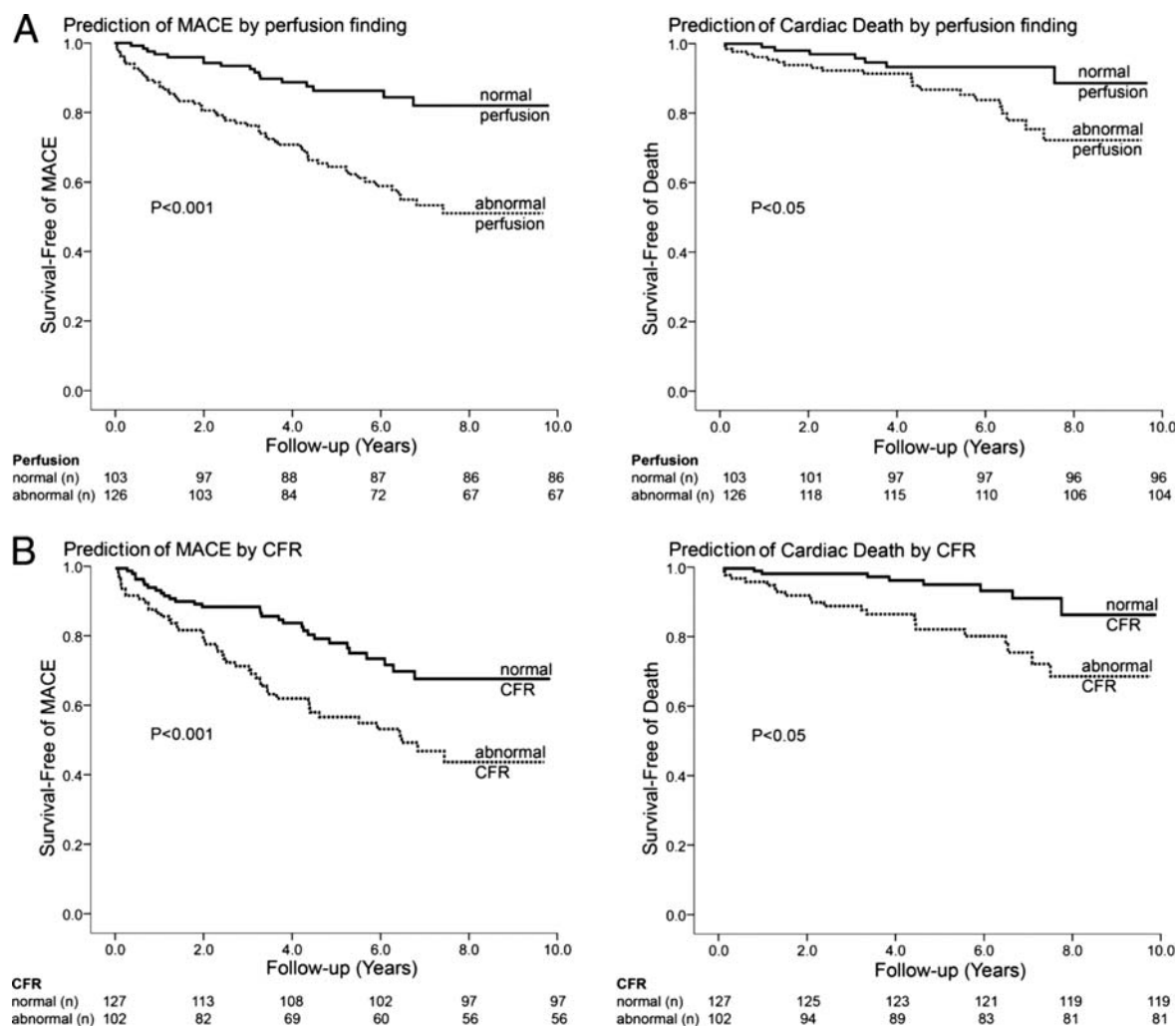


**Figure 3** Kaplan–Meier survival curves (unadjusted) showing prognostic value of coronary flow reserve in patients with abnormal vs. normal perfusion. (A) Coronary flow reserve predicts major adverse cardiac events (left) and cardiac death (right) in patients with abnormal perfusion findings. (B) The prognostic value of coronary flow reserve to predict major adverse cardiac events (left) and cardiac death (right) in patients with normal perfusion is confirmed to the first 3 years; survival curves merge throughout the subsequent years of follow-up. Herzog *et al.*,<sup>34</sup> with permission.

A number of different techniques, including PET, have been used to investigate the mechanisms of myocardial hibernation and tissue viability before revascularization.<sup>47,48</sup> A unifying feature of most available studies is the demonstration that a severe reduction in CFR is the common pathophysiological predecessor for both stunning and hibernation.<sup>49</sup> Repeated episodes of demand ischaemia may lead to cumulative stunning that could be a predecessor of chronic post-ischaemic LV dysfunction.<sup>44</sup> Hibernation is now believed to be the consequence of repetitive bouts of ischaemia and stunning (chronic stunning hypothesis) due to normally occurring increases in myocardial metabolic demand in the face of significant coronary stenoses and limited CFR.<sup>49</sup> Indeed, recovery of function in hibernating myocardium requires coronary revascularization which in turn restores an adequate CFR<sup>47</sup> (Figure 4). In addition, a novel mechanism underlying hibernating myocardium, in the form of an endogenous genomic cytoprotection that

could subtend cell survival under conditions of prolonged ischaemia, has been demonstrated both in animal models and patients<sup>50</sup> (Figure 5).

### Positron emission tomography metabolic tracers

PET metabolic tracers include markers of: (i) glucose utilization and metabolism: <sup>18</sup>F-FDG and <sup>11</sup>C-glucose; (ii) fatty acid metabolism: <sup>11</sup>C-palmitate, <sup>18</sup>F-fluoro-6-thia-heptadecanoic acid and <sup>18</sup>F-16-fluoro-4-thia-palmitate (FTP); and (iii) oxidative and oxygen metabolism: <sup>11</sup>C-acetate and <sup>15</sup>O<sub>2</sub> (Figure 1). With the exception of <sup>18</sup>F-FDG, these tracers are primarily experimental. Our discussion focuses on <sup>18</sup>F-FDG PET.

To date, the most widely used and validated PET radiotracer for the assessment of myocardial glucose utilization and

metabolically active viable tissue is <sup>18</sup>FDG.<sup>47,51–53</sup> <sup>18</sup>FDG is a glucose analogue in which the 1-OH group is replaced by an <sup>18</sup>F atom. The tracer is transported into the myocyte by the

same sarcolemmal glucose transporters (GLUT1 and GLUT4) as glucose and phosphorylated to <sup>18</sup>FDG-6-phosphate by hexokinase. This is essentially a unidirectional reaction, because the appropriate phosphatase to convert <sup>18</sup>FDG-6-phosphate back to free <sup>18</sup>FDG is not present in myocardium (Figure 1). There is, therefore, an increase in <sup>18</sup>FDG-6-phosphate within the myocyte over time that is proportional to the overall rate of trans-sarcolemmal transport and the activity of hexokinase. However, unlike glucose, <sup>18</sup>FDG is not further metabolized or used for glycogen storage and remains trapped in the myocyte as <sup>18</sup>FDG-6-phosphate.<sup>54</sup> In the fasting state, <sup>18</sup>FDG uptake is low reflecting the low glucose uptake and oxidation. After oral carbohydrate loading, myocardial uptake of <sup>18</sup>FDG is high reflecting increased myocardial glucose utilization due to the release of endogenous insulin, which inhibits FFA release from adipocytes leading to reduced circulating FFA.<sup>55</sup> Thus, to improve diagnostic quality by enhancing myocardial FDG uptake, several methods have been employed including oral glucose loading or infusion of insulin and glucose. These methods are briefly summarized below, but can be found in more details in the guidelines of the ASNC.<sup>15</sup>

A small number of laboratories have applied <sup>11</sup>C-acetate in the clinical setting, but its use primarily remains investigational.<sup>22,56,57</sup>

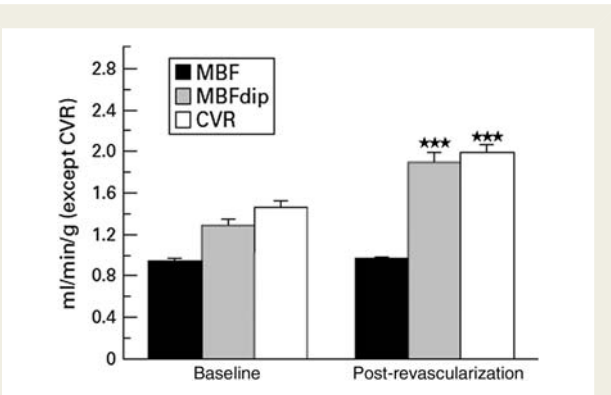


**Figure 4** Perfusion data on 163 hibernating myocardial segments before (baseline) and after coronary revascularization. MBF, myocardial blood flow; MBFdip, post-dipyridamole myocardial blood flow; CVR, coronary vasodilator reserve. \*\*\**P* < 0.0001. Reprinted from Pagano et al.<sup>96</sup> with permission.

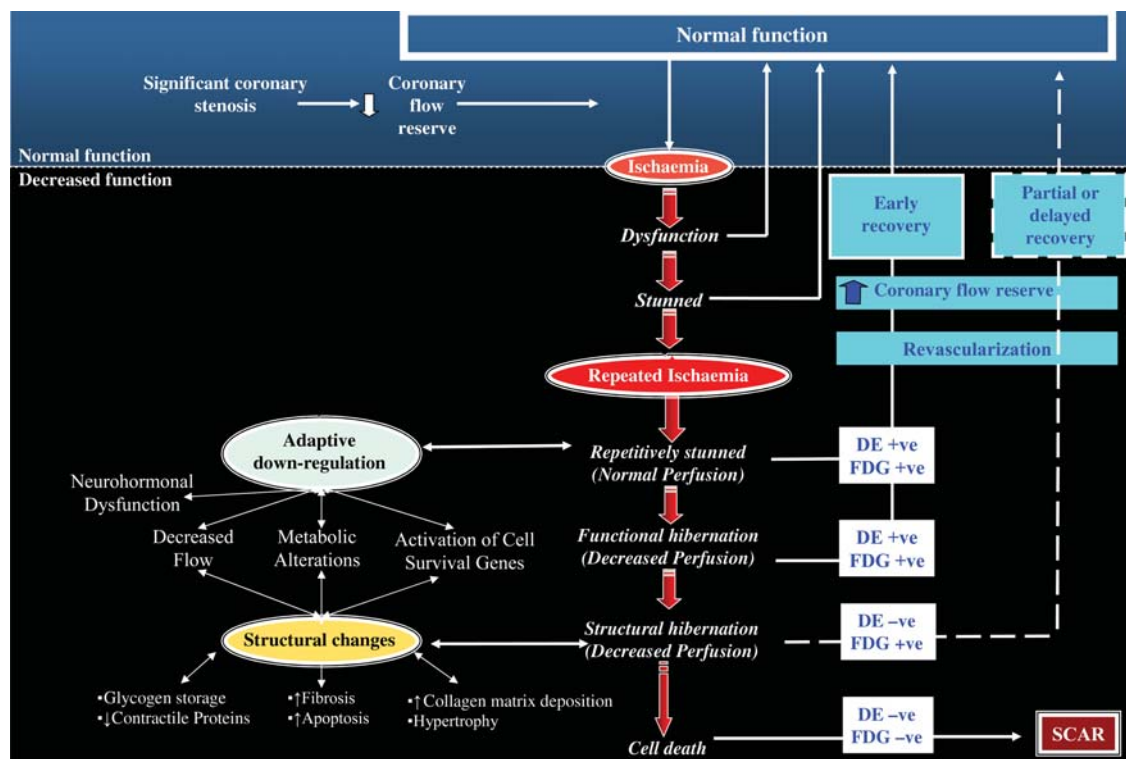


**Figure 5** Proposed mechanisms underlying hibernating myocardium (see text for more details). There is progression from repetitive stunning and functional hibernation (associated with little structural change and prompt recovery with revascularization) to structural hibernation (with glycogen accumulation and loss of contractile elements, which recovers slowly or incompletely after revascularization) and if untreated progresses to irreversible injury, which leads to scar formation. As myocytes become increasingly deranged, their contractile reserve and hence their ability to respond to dobutamine, is lost (DE-ve); while some metabolic activity must be maintained to sustain cell viability. Hence FDG is still taken up by the myocytes (FDG+ve). FDG, fluorodeoxyglucose; DE, dobutamine echocardiogram. Adapted from Camici and Dutka<sup>97</sup> and Beanlands et al.,<sup>60</sup> with permission.

## Viability imaging using perfusion and $^{18}\text{F}$ -fluorodeoxyglucose

Ischaemic cardiomyopathy continues to be the most common aetiology for myocardial dysfunction in developed countries.<sup>58</sup> The assessment of myocardial viability with  $^{18}\text{F}$ FDG PET is based on its ability to distinguish between the two main pathogenic mechanisms for chronic myocardial dysfunction in ischaemic cardiomyopathy: (i) irreversible loss of myocardium due to prior myocardial infarction (scar) and (ii) at least partially reversible loss of contractility as a result of chronic or repetitive ischaemia (hibernating myocardium). The distinguishing feature of these two mechanisms is that revascularization has the potential to restore contractile function of hibernating myocardium but not scar. This distinction may be crucially important in clinical decision-making because of the upfront morbidity and mortality associated with revascularization procedures in patients with severe LV dysfunction.

Traditional  $^{18}\text{F}$ FDG-PET myocardial viability assessment requires integration of rest perfusion imaging with myocardial glucose metabolism imaging. Positron emission tomography MPI is preferable to SPECT for comparison with  $^{18}\text{F}$ FDG metabolism images because of limitations imposed by differences in attenuation correction algorithms.<sup>15,59–61</sup> Positron emission tomography MPI studies are acquired at rest with standard perfusion protocols and compared with  $^{18}\text{F}$ FDG.<sup>51–53,62</sup> For  $^{18}\text{F}$ FDG imaging, patients are generally studied after an oral glucose load. If the patient has glucose intolerance or diabetes, supplemental insulin will be required. Alternatively, some centres routinely employ the hyperinsulinemic euglycemic clamp or use it preferentially in patients with diabetes.<sup>15,59,60,63</sup>

Comparison of perfusion and metabolism images can yield one of four common patterns (see Table 1).

Normal myocardium has preserved myocardial perfusion and metabolism.

In the *perfusion-metabolism mismatch* pattern, perfusion is reduced whereas metabolism ( $^{18}\text{F}$ FDG uptake) is preserved (Figure 6). This pattern has been considered the hallmark of myocardial hibernation.<sup>15,60</sup> Higher degrees of mismatch have been shown to be associated with improved LV function with revascularization.<sup>51,64</sup> Di Carli et al.<sup>65</sup> demonstrated that when hibernation was present in as little as 5% of the myocardium, an outcome benefit from revascularization could be demonstrated. This observation was recently supported in a *post hoc* analysis of the

**Table 1** Simplified classification system for flow-metabolism patterns in  $^{18}\text{F}$ -fluorodeoxyglucose-positron emission tomography myocardial viability studies (see text for details)

Perfusion	Glucose metabolism	Category
Preserved	Preserved	(Viable)
Reduced	Preserved	Mismatch (viable hibernation)
Reduced	Reduced	Match (non-viable)
Preserved	Reduced	Reverse mismatch (altered regional glucose metabolism)

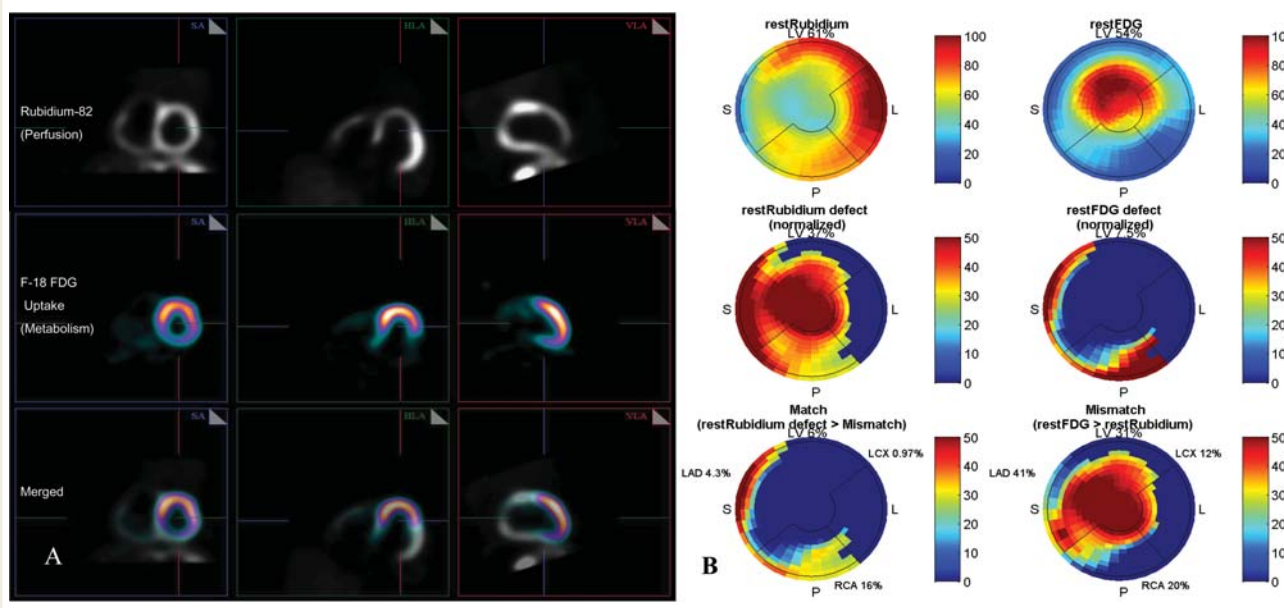


**Figure 6**  $^{18}\text{F}$ -fluorodeoxyglucose-positron emission tomography myocardial viability scan showing mismatch pattern. (A) The rest rubidium perfusion images. There is reduction in uptake in the anterior wall and apex (top row). The  $^{18}\text{F}$ -fluorodeoxyglucose metabolism images (middle row) show significant  $^{18}\text{F}$ -fluorodeoxyglucose uptake in the anterior wall and apex, indicating there is significant perfusion-metabolism mismatch, or hibernating myocardium in these regions as is seen more clearly in the merged images (bottom row). (B) The quantified mismatch score (31% of the left ventricle) and match score (6% of the left ventricle). Panel (A) reprinted from Gropler et al.<sup>98</sup> Panel (B) reproduced by permission of the creators J. Renaud and R. deKemp.

prospective randomized trial, PET and Recovery Following Revascularization-2 (PARR-2) trial. D'Egidio *et al.*<sup>66</sup> identified a cutoff of >7% mismatch as an indicator that patients with ischaemic cardiomyopathy would have outcome benefit from revascularization (Figure 7).

In a recent meta-analysis, the optimal threshold for the presence of viability required to improve *survival* with revascularization was estimated to be 25.8% (95% CI: 16.6–35.0%) by <sup>18</sup>F-DG PET perfusion mismatch for the assessment of viability.<sup>67</sup>

In the *perfusion-metabolism match* pattern, there is both reduced perfusion and reduced metabolism (Figure 8). This pattern is indicative of myocardium that is predominantly scar. The extent of scar has also been shown to be important in the prediction of LV function recovery after revascularization. Ottawa investigators showed that *quantification* of scar was an independent predictor of improvement of LV function following revascularization in a cohort of patients with severe LV dysfunction. Specifically, across tertiles of scar scores [small (0–16% scar); moderate (16–27.5%); large (27.5–45%)], changes in EF post-revascularization were 9, 3.7, and 1.3%, respectively.<sup>68</sup>

Finally, the *reverse mismatch pattern* denotes normal perfusion with relatively reduced metabolism. This pattern can be observed in several settings, including in patients with: non-ischaemic cardiomyopathy, left bundle branch block (LBBB), repetitive stunning, following revascularization early post-MI when the myocardium is stunned, and in some patients with diabetes. Reverse mismatch with LBBB has been suggested to be a consequence of altered septal glucose metabolism.<sup>69</sup> Recent evidence suggests that the presence of reverse mismatch (as well as the extent of lateral scar and the overall extent of viability), on perfusion/<sup>18</sup>F-DG PET imaging can be used to predict outcome response in patients undergoing cardiac resynchronization

therapy.<sup>70–72</sup> The clinical significance of the reverse mismatch pattern itself warrants further investigation.

### Viability imaging using <sup>18</sup>F-DG alone and euglycemic hyperinsulinemic clamp

The semi-quantitative and quantitative analyses of <sup>18</sup>F-DG uptake may enhance detection of viable myocardium at the price of a rigorous standardization of the study conditions.<sup>73</sup> Many patients with CAD are insulin resistant, i.e. the amount of endogenous insulin released after feeding will not induce maximal stimulation due to partial resistance of the myocytes to the action of the hormone even if they are not diabetic.<sup>74</sup> This may often result in poor <sup>18</sup>F-DG image quality after an oral glucose load. To circumvent the problem of insulin resistance, the hyperinsulinemic euglycemic clamp protocol has been applied to PET viability studies.<sup>75</sup> This protocol is based on the simultaneous infusion of insulin and glucose acting on the tissue as a metabolic challenge and stimulating maximal <sup>18</sup>F-DG uptake. The use of the euglycemic hyperinsulinemic glucose clamp provides excellent image quality, usually demonstrates uniform tracer uptake and enables PET studies to be performed under steady and standardized metabolic conditions. If a fully quantitative analysis is carried out it is possible to compare absolute values of the metabolic rate of glucose uptake ( $\mu\text{mol/g/min}$ ) among different subjects and centres.

A significant benefit of full quantification is its sensitivity in patients with CAD and poor LV function. Using this approach, Hammersmith Hospital investigators have studied a large series of patients undergoing revascularization procedures and have demonstrated good predictive accuracy of PET under different clinical conditions. A threshold value for the metabolic rate of

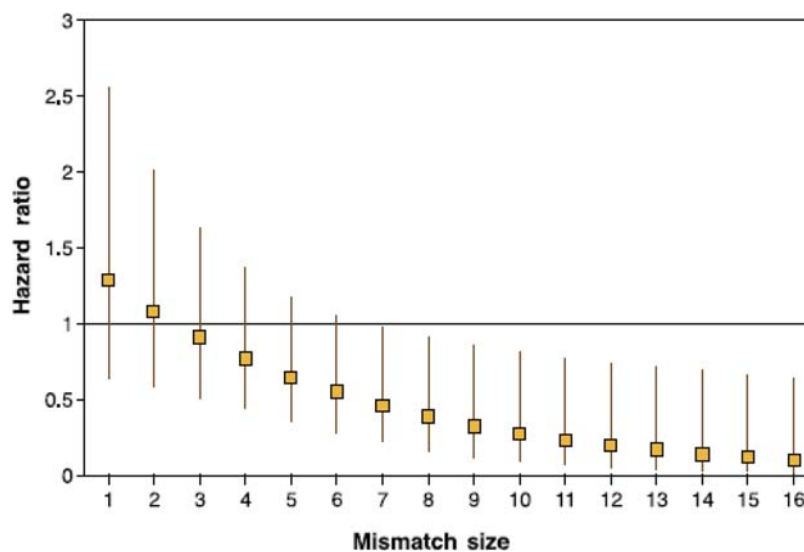


**Figure 7** Interaction hazard ratios and 95% confidence interval at various levels of mismatch measured as a continuous variable. D'Egidio *et al.* showed that, for those with <sup>18</sup>F-fluorodeoxyglucose-positron emission tomography perfusion/metabolism mismatch of <7% there is no significant difference in the risk of the primary outcome if revascularization is done compared with not done. As mismatch increases (i.e.  $\geq 7\%$ ), they observed a decreased risk of the primary outcome for those who undergo revascularization. For those with mismatch of 7%, there is a 0.46 times lower risk for the primary outcome if revascularization is done. From D'Egidio *et al.*,<sup>66</sup> with permission.



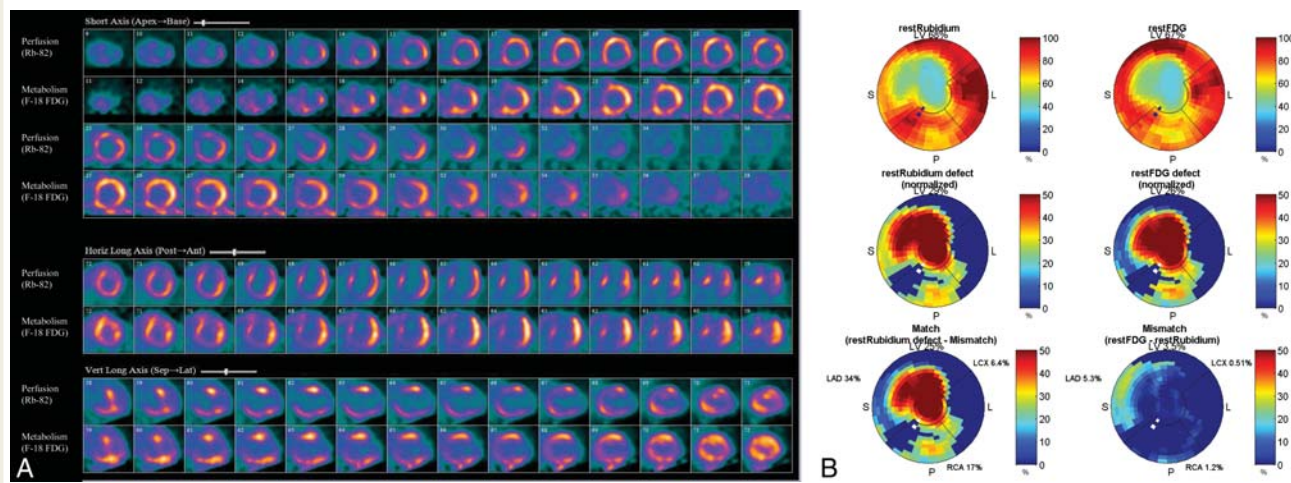


**Figure 8**  $^{18}\text{F}$ -fluorodeoxyglucose-positron emission tomography viability scan showing match pattern: (A) The rest perfusion  $^{82}\text{Rb}$  images. There is significant reduction in uptake in the anteroseptal wall and apex. The  $^{18}\text{F}$ -fluorodeoxyglucose metabolism images show corresponding reduction in  $\text{F-}^{18}\text{F}$ -fluorodeoxyglucose uptake in the anteroseptal wall and apex, indicating there is perfusion-metabolism match, or scar in these regions. (B) The quantified mismatch score was 3.5% of the left ventricle and match score was 25% of the left ventricle. LV, left ventricle; LAD, left anterior descending; LCX, left circumflex; RCA, right coronary artery.

glucose of  $0.25 \mu\text{mol/g/min}$  corrected for perfusable tissue fraction, allowed the best prediction of improvement in functional class of at least one grade after revascularization.<sup>76</sup> Lautamaki et al.<sup>77</sup> reported similar values in a population of patients with Type 2 diabetes and CAD; during insulin stimulation they found that myocardial glucose uptake in ischaemic regions was similar to that of non-ischaemic regions.

While accuracy data have yielded results that are similar to perfusion/metabolism mismatch for predicting LV function recovery, most of the outcome data has applied perfusion/metabolism imaging approach. Currently the ASNC guidelines recommend the use of perfusion with  $^{18}\text{F}$ FDG to assist in defining the perfusion/metabolism mismatch pattern, the hallmark of hibernation and the parameter most related to patient risk for adverse outcomes if they do not undergo revascularization.

### Prospective data on the utility of $^{18}\text{F}$ -fluorodeoxyglucose-positron emission tomography on assessment of myocardial viability

$^{18}\text{F}$ -fluorodeoxyglucose imaging is considered to be the most sensitive means to measure myocardial viability. Several investigations have reported good accuracy of  $^{18}\text{F}$ FDG imaging in predicting improvement in LV function after revascularization.<sup>48,51,59,64,78–81</sup> A recent systematic review by Schinkel et al.<sup>48</sup> demonstrated that  $^{18}\text{F}$ FDG PET is more sensitive than any other viability imaging modality (Figure 9). A recent health technology assessment identified the pooled estimates of sensitivity and specificity of  $^{18}\text{F}$ FDG PET for predicting wall motion recovery to be 91.5 and 67.8%, respectively.<sup>82</sup>

Several observational studies have shown that  $^{18}\text{F}$ FDG PET is important for prognostication of patients with viable myocardium

who do not undergo timely revascularization.<sup>48,65,83–86</sup> However, only recently has the impact of  $^{18}\text{F}$ FDG viability imaging in clinical decision-making and its effect on patient outcome been evaluated. A patient-outcome oriented approach to imaging is particularly crucial in a contemporary era of rapidly proliferating imaging techniques and in the setting of resource limitations imposed by health-care economic realities.

Siebelink et al.<sup>82</sup> performed a randomized controlled trial comparing  $^{99\text{m}}\text{Tc}$ -sestamibi SPECT to  $^{13}\text{NH}_3/^{18}\text{F}$ FDG PET in 103 patients. The PET arm had slightly fewer events but there was no significant difference in outcomes. However, only approximately one-third of these 103 patients had severe LV dysfunction (those most likely to benefit from revascularization). In addition there were long delays to revascularization, which may limit the benefit of viability imaging in many patients and therefore may have made the study unable to detect differences. Prior studies have shown that benefits for revascularization may be lost if there are excessive delays to revascularization.<sup>87,88</sup> These limitations make it difficult to extrapolate data from this study regarding the viability detection in patients with severe LV dysfunction.

The PET and PARR-2 study was a randomized controlled trial conducted to ascertain whether the use of  $^{18}\text{F}$ FDG PET in clinical decision-making resulted in better clinical outcome compared with standard care where PET was not available. This was a multi-centre trial in patients with a LVEF  $\leq 35\%$  due to suspected coronary artery disease, who were being considered for revascularization, transplantation or heart failure work-up. In the PET arm, extent and severity of scar and mismatch were determined and considered in the context of a previously derived model to predict LV recovery after revascularization. Using the results of this model and the interpretation of PET images, the physician and surgeon would decide on whether or not to proceed with revascularization or revascularization work-up. Although there

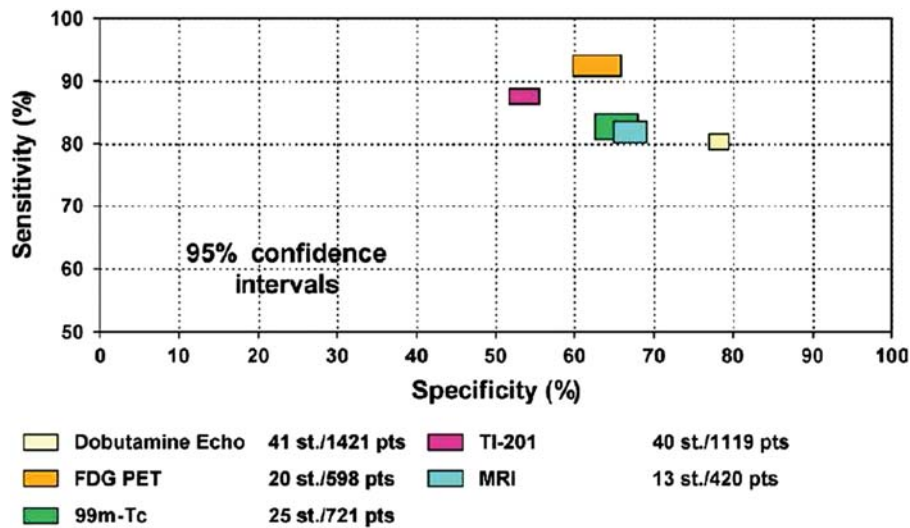


**Figure 9** Comparison of sensitivities and specificities with 95% confidence intervals of the various techniques for the prediction of recovery of regional function after revascularization.  $^{18}\text{F}$ -fluorodeoxyglucose positron emission tomography viability was shown to have the greatest sensitivity, while dobutamine echocardiography was shown to have the greatest specificity for predicting recovery of regional function after revascularization. From Schinkel *et al.*<sup>48</sup>, with permission.

was a trend for better outcomes using the PET strategy compared with standard care, overall the trial was inconclusive as there was no statistically significant difference between the two groups. However, in a *post hoc* analysis that compared those that adhered to PET recommendations ('ADHERE' arm), there was a significant decrease in the hazard ratio for the primary outcome compared with standard care (Figure 10). Further *post hoc* analysis revealed there was a benefit of  $^{18}\text{F}$ FDG PET in an experienced centre with ready access to and routine integration of  $^{18}\text{F}$ FDG PET, which may facilitate clinical decision-making.<sup>66</sup>

Taken together, the findings of the PARR-2 trial, its sub-studies and other outcome observational data, support that  $^{18}\text{F}$ FDG-PET viability imaging has clinical utility in identifying high-risk patients who may benefit from revascularization and is a valuable tool in improving patient outcomes if  $^{18}\text{F}$ FDG-based recommendations can be meaningfully incorporated into an overall management strategy. Further randomized trials incorporating viability imaging as part of the work up for management of ischaemic cardiomyopathy, which go beyond the observational studies that have populated much of the viability research to date, are still required to truly appreciate the clinical value of these imaging techniques. Trials such as IMAGE-HF are now underway and plan to address these questions.

### Relative merit of $^{18}\text{F}$ -fluorodeoxyglucose-positron emission tomography viability imaging vs. other modalities for assessing viability

$^{18}\text{F}$ -fluorodeoxyglucose-positron emission tomography defines metabolic cell integrity and has the highest sensitivity compared with other methods for prediction of segmental contractile function recovery, whereas techniques challenging contractile reserve

such as dobutamine stress with echocardiogram (DSE) or cardiac magnetic resonance (CMR) showed the highest specificity.<sup>48</sup> This is also exemplified in Figure 5. The ability of different imaging modalities to predict the recovery of LV function after revascularization in a population with a prevalence of viability assessed by the optimal cutoff (i.e. number of viable segments) identified by the receiver operating curve (ROC) analysis confirm that SPECT and PET have higher sensitivity and DSE has superior specificity and lower PPV.<sup>47</sup>

The importance of the cutoff value has been further highlighted in a recent paper by Inaba *et al.*<sup>67</sup> The amount of myocardium deemed necessary for improvement of survival with revascularization was characteristic of each technique. Positron emission tomography requires the least amount of viable myocardium (25.8%) in comparison with DSE (35.9%) and SPECT (38.7%) (Table 2). Caution is of the essence when evaluating meta-analyses results and some limitations must be taken into consideration. As noted by the authors the optimal cutoff for viability with different modalities was based on the assumption of a linear relationship between viability and survival. Also the studies used observational data which is fraught with biased. The authors note recent work by D'Egidio *et al.*<sup>66</sup> not included in their analysis, in which as little as 7% of the myocardium as mismatch may be needed to yield an outcome benefit from revascularization (outcome was cardiac death, MI, and cardiac hospitalization). This cutoff is similar to early work by Di Carli *et al.*<sup>65</sup> and Lee *et al.*<sup>89</sup> who used 5% (1/20 segments) and 7.6% (1/13), respectively, as the cutoff to define significant viability. Other limitations of meta-analysis include the heterogeneity of the criteria used in different centres, the different duration of the follow-up, the lag between viability assessment and revascularization, the extent of LV remodelling, co-morbidities preventing timely revascularization, failure

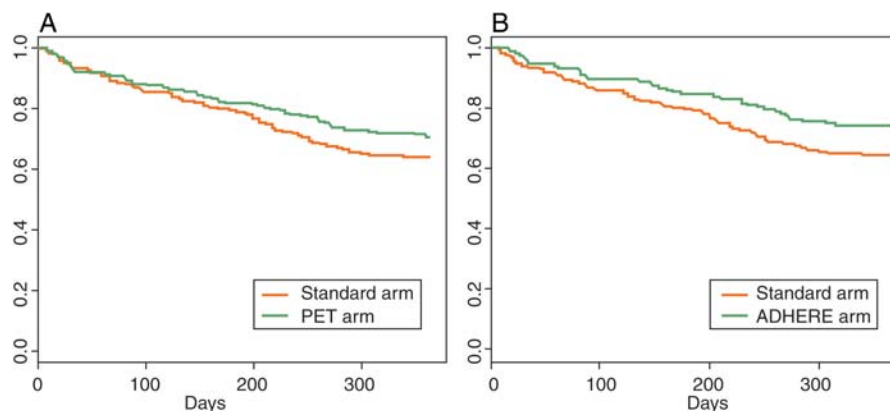


**Figure 10** Clinical impact of  $^{18}\text{F}$ -fluorodeoxyglucose viability studies in the PARR-2 study. Survival curves for the composite outcome (a composite of cardiac death, myocardial infarction, or recurrent hospital stay for cardiac cause), within 1 year in the overall study (A) and in the *post hoc* analysis comparing patients where positron emission tomography recommendations were adhered to, versus the standard arm (B). The hazard ratio (HR) for the composite outcome, positron emission tomography vs. standard care, was 0.78 (95% CI: 0.58–1.1;  $P = 0.15$ ); for patients that adhered to positron emission tomography recommendations for revascularization, revascularization work-up, or neither, HR = 0.62 (95% CI: 0.42–0.93;  $P = 0.019$ ); in those without recent angiography, for cardiac death, HR = 0.4 (95% CI: 0.17–0.96;  $P = 0.035$ ). From Beanlands et al.,<sup>53</sup> – with permission.

**Table 2** Optimal cutoff values for the presence of viability leading to improved survival with revascularization over medical therapy

Imaging techniques (number of studies)	Mean viable myocardium, SD (%)	Optimal threshold for viability (%)
PET overall ( $n = 7$ )	21 (13)	25.8 (16.6–35.0)
PET with FDG/ $\text{NH}_3$ ( $n = 3$ )	20 (15)	22.5 (10.1–34.8)
PET with FDG/ $\text{Tc-99m}$ ( $n = 3$ )	22 (16)	29.2 (20.7–37.8)
Stress echo overall ( $n = 8$ )	32 (24)	35.9 (31.6–40.3)
Stress echo with LDDE ( $n = 4$ )	33 (28)	33.6 (27.4–39.8)
Stress echo with HDDE ( $n = 2$ )	35 (31)	44.1 (37.2–50.9)
SPECT overall ( $n = 6$ )	38 (25)	38.7 (27.7–49.7)
SPECT with $\text{Tl-201}$ ( $n = 5$ )	41 (35)	38.0 (26.2–49.7)

Echo, echocardiography; FDG, fluorine-18 fluorodeoxyglucose; HDDE, high-dose dobutamine echocardiography; LDDE, low-dose dobutamine echocardiography;  $^{13}\text{NH}_3$ , nitrogen-13 ammonia; PET, positron emission tomography; SD, standard deviation;  $\text{Tc-99}$ , technetium-99m; and  $\text{Tl-201}$ , thallium-201. From Inaba et al.,<sup>67</sup> with permission.

of revascularization procedures, and adherence to current guidelines for medical therapy. Regarding CMR, a highly sensitive method to detect scarred myocardium, limited data are available so far on the prognostic value.<sup>90</sup>

## Summary and concluding remarks

Although coronary revascularization is performed frequently, its role, especially in patients with moderate-to-severe LV

dysfunction, who do not have angina or reversible myocardial ischaemia, remains uncertain.<sup>91</sup> Recent European Guidelines on Heart Failure do not clearly recommend revascularization as a specific intervention in patients with chronic ischaemic LV dysfunction unless they suffer from angina.<sup>92</sup> This is due to the lack of specific randomized trials comparing the value of coronary revascularization when added to optimal medical therapy.

At present only one ongoing randomized trial is tackling this specific issue, i.e. the Surgical Treatment for Ischemic Heart Failure (STICH) Trial.<sup>93</sup> The STICH primary hypothesis is that improvement in myocardial perfusion by coronary artery bypass surgery (CABG) combined with optimal medical therapy improves long-term survival. A sub-study that will be announced in 2012, deals with the identification of patients with greatest survival advantage based on the presence and extent of dysfunctional, but viable myocardium, as defined by non-invasive imaging (ClinicalTrials.gov Identifier: NCT00023595).

Coronary artery bypass surgery in patients with severe LV systolic dysfunction is associated with higher peri-procedural complications and mortality (~3% stroke, ~5% death within 30 days post-surgery).<sup>94</sup> Furthermore, recent studies provide evidence that percutaneous coronary interventions (PCI) can be used safely to achieve complete revascularization in patients with severe CAD.<sup>95</sup> Although the STICH trial will add valuable information to improve the therapeutical strategies in patients with chronic systolic LV dysfunction due to CAD, important issues will remain unresolved. In particular, in STICH, PCI was considered part of the medical stratum, despite its effective restoration of flow with lower peri-procedural morbidity and mortality compared with CABG.<sup>95</sup> Furthermore, in the STICH trial, viability was not assessed in all patients recruited nor was it used to direct therapy. In those in whom viability was evaluated, different methods were used that might lead to variability in the accuracy of its detection.

In conclusion, further randomized trials will be needed to conclusively assess whether routine assessment of myocardial viability before revascularization can: (a) identify those patients who might benefit most from revascularization; (b) choose the most appropriate revascularization approach; (c) avoid unnecessary procedures and risk in those patients with minimal or absent viability.

## Funding

The National Cardiac PET Centre, Division of Cardiology and the Molecular Function and Imaging Programme is supported in part by Heart and Stroke Foundation of Ontario (# PRG6242). R.B. is a Career Investigator supported by the Heart and Stroke Foundation of Ontario.

**Conflict of interest:** R.B. is a consultant with Lantheus Medical Imaging and DraxImage. He has received industry/government grant funding from GE and MDS Nordion. N.G. has no conflicts of interest. O.R. has no conflicts of interest. P.C. works as consultant for Servier International and has received industry funding from GE.

## References

- Rosamond W, Flegal K, Furie K, Go A, Greenlund K, Haase N, Hailpern SM, Ho M, Howard V, Kissela B, Kittner S, Lloyd-Jones D, McDermott M, Meigs J, Moy C, Nichol G, O'Donnell C, Roger V, Sorlie P, Steinberger J, Thom T, Wilson M, Hong Y. Heart disease and stroke statistics—2008 update: a report from the American Heart Association Statistics Committee and Stroke Statistics Subcommittee. *Circulation* 2008;**117**:e25–e146.
- US Food & Drug Administration. Technetium-99m radiopharmaceutical product shortage. <http://www.fda.gov/Drugs/DrugSafety/PostmarketDrugSafetyInformationforPatientsandProviders/ucm176226.htm> (6 July 2010).
- Camici PG, Rimoldi OE. The clinical value of myocardial blood flow measurement. *J Nucl Med* 2009;**50**:1076–1087.
- Dobrucki LW, Sinusas AJ. PET and SPECT in cardiovascular molecular imaging. *Nat Rev Cardiol* 2010;**7**:38–47.
- Schelbert HR. Metabolic imaging to assess myocardial viability. *J Nucl Med* 1994;**35**(4 Suppl.):85–145.
- Bengel FM, Higuchi T, Javadi MS, Lautamaki R. Cardiac positron emission tomography. *J Am Coll Cardiol* 2009;**54**:1–15.
- Knuuti J, Schelbert HR, Bax JJ. The need for standardisation of cardiac FDG PET imaging in the evaluation of myocardial viability in patients with chronic ischaemic left ventricular dysfunction. *Eur J Nucl Med Mol Imaging* 2002;**29**:1257–1266.
- Krivokapich J, Smith GT, Sung-Cheung H, Hoffman EJ, Osman R, Phelps ME, Schelbert HR. 13-N ammonia myocardial imaging at rest and with exercise in normal volunteers; Quantification of absolute myocardial perfusion with dynamic positron emission tomography. *Circulation* 1989;**80**:1328–1337.
- Araujo LI, Lammertsma AA, Rhodes CG, McFalls EO, Iida H, Rechavia E, Galassi A, De Silva R, Jones T, Maseri A. Noninvasive quantification of regional myocardial blood flow in normal volunteers and patients with coronary artery disease using oxygen-15 labeled water and positron emission tomography. *Circulation* 1991;**83**:875–885.
- Bassingthwaite JB, Beard DA. Fractal 15O-labeled water washout from the heart. *Circ Res* 1995;**77**:1212–1221.
- Rimoldi O, Schafers KP, Boellaard R, Turkheimer F, Stegger L, Law MP, Lammertsma AA, Camici PG. Quantification of subendocardial and subepicardial blood flow using 15O-labeled water and PET: experimental validation. *J Nucl Med* 2006;**47**:163–172.
- Di Carli MF, Dorbala S. Cardiac PET-CT. *J Thorac Imaging* 2007;**22**:101–106.
- Souvatoglou M, Bengel F, Busch R, Kruschke C, Fernolendt H, Lee D, Schwaiger M, Nekolla SG. Attenuation correction in cardiac PET/CT with three different CT protocols: a comparison with conventional PET. *Eur J Nucl Med Mol Imaging* 2007;**34**:1991–2000.
- Lubberink M, Harms HJ, Halbmeijer R, de Haan S, Knaapen P, Lammertsma AA. Low-dose quantitative myocardial blood flow imaging using 15O-water and PET without attenuation correction. *J Nucl Med* 2010;**51**:575–580.
- Dilsizian V, Bacharach SL, Beanlands RS, Bergmann SR, Delbeke D, Gropler RJ, Knuuti J, Schelbert HR, Travin MI. PET myocardial perfusion and metabolism clinical imaging. *J Nucl Cardiol* 2009;**16**:651.
- Bateman TM, Heller GV, McGhie AI, Friedman JD, Case JA, Bryngelson JR, Hertenstein GK, Moutray KL, Reid K, Cullom SJ. Diagnostic accuracy of rest/stress ECG-gated Rb-82 myocardial perfusion PET: comparison with ECG-gated Tc-99m sestamibi SPECT. *J Nucl Cardiol* 2006;**13**:24–33.
- Lalonde L, Ziadi MC, Beanlands R. Cardiac positron emission tomography: current clinical practice. *Cardiol Clin* 2009;**27**:237–255.
- Ziadi MC, deKemp R, Yoshinaga K, Beanlands R. Myocardial perfusion and flow with PET. In: Zaret B, Beller G, eds. *Clinical Nuclear Cardiology: State of the Art and Future Directions*. 4th ed. Philadelphia: Mosby Elsevier; 2010.
- Go RT, Marwick TH, MacIntyre WJ, Saha GB, Neumann DR, Underwood DA, Simpfordorfer CC. A prospective comparison of rubidium-82 PET and thallium-201 SPECT myocardial perfusion imaging utilizing a single dipyridamole stress in the diagnosis of coronary artery disease. *J Nucl Med* 1990;**31**:1899–1905.
- Stewart R, Schwaiger M, Molina M, Popma J, Gacioh G, Kalus M, Squicciarini S, Al-Aouar Z, Schork A, Kuhl D. Comparison of rubidium-82 positron emission tomography and thallium-201 SPECT imaging for detection of coronary artery disease. *Am J Cardiol* 1991;**67**:1303–1310.
- Marwick TH, Shan K, Patel S, Go RT, Lauer MS. Incremental value of rubidium-82 positron emission tomography for prognostic assessment of known or suspected coronary artery disease. *Am J Cardiol* 1997;**80**:865–870.
- Yoshinaga K, Chow BJ, Williams K, Chen L, deKemp RA, Garrard L, Lok-Tin SA, Aung M, Davies RA, Ruddy TD, Beanlands RS. What is the prognostic value of myocardial perfusion imaging using rubidium-82 positron emission tomography? *J Am Coll Cardiol* 2006;**48**:1029–1039.
- Dorbala S, Hachamovitch R, Curillova Z, Thomas D, Vangala D, Kwong RY, Di Carli MF. Incremental prognostic value of gated Rb-82 positron emission tomography myocardial perfusion imaging over clinical variables and rest LVEF. *JACC Cardiovasc Imaging* 2009;**2**:846–854.
- Lertsburapa K, Ahlberg AW, Bateman TM, Katten D, Volker L, Cullom SJ, Heller GV. Independent and incremental prognostic value of left ventricular ejection fraction determined by stress gated rubidium 82 PET imaging in patients with known or suspected coronary artery disease. *J Nucl Cardiol* 2008;**15**:745–753.
- Uren NG, Melin JA, De Bruyne B, Wijns W, Baudhuin T, Camici PG. Relation between myocardial blood flow and the severity of coronary artery stenosis. *N Engl J Med* 1994;**330**:1782–1788.
- Di Carli M, Czernin J, Hoh CK, Gerbaudo VH, Brunken RC, Huang SC, Phelps ME, Schelbert HR. Relation among stenosis severity, myocardial blood flow, and flow reserve in patients with coronary artery disease. *Circulation* 1995;**91**:1944–1951.
- Choudhury L, Rosen SD, Patel D, Nihoyannopoulos P, Camici PG. Coronary vasodilator reserve in primary and secondary left ventricular hypertrophy. A study with positron emission tomography. *Eur Heart J* 1997;**18**:108–116.
- Sdringola A, Dhaval P, Gould KL. High prevalence of myocardial perfusion abnormalities on positron emission tomography in asymptomatic persons with a parent or sibling with coronary artery disease. *Circulation* 2001;**103**:496–501.
- Rajappan K, Rimoldi O, Dutka D, Ariff B, Pennell D, Sheridan D, Camici P. Mechanism of coronary microcirculatory dysfunction in patients with aortic stenosis and angiographically normal coronary arteries. *Circulation* 2002;**105**:470–476.
- Radvan J, Choudhury L, Sheridan DJ, Camici PG. Comparison of coronary vasodilator reserve in elite rowing athletes versus hypertrophic cardiomyopathy. *Am J Cardiol* 1997;**80**:1621–1623.
- Rosen S, Uren NG, Kaski J-C, Tousoulis D, Davies G, Camici P. Coronary vasodilator reserve, pain perception, and sex in patients with syndrome X. *Circulation* 1994;**90**:50–60.
- Chareonthaitawee P, Kaufmann PA, Rimoldi O, Camici PG. Heterogeneity of resting and hyperemic myocardial blood flow in healthy humans. *Cardiovasc Res* 2001;**50**:151–161.
- Tio RA, Dabeshlim A, Siebelink HM, de Sutter J, Hillege HL, Zeebregts CJ, Dierckx RA, van Veldhuisen DJ, Zijlstra F, Slart RH. Comparison between the prognostic value of left ventricular function and myocardial perfusion reserve in patients with ischemic heart disease. *J Nucl Med* 2009;**50**:214–219.
- Herzog BA, Husmann L, Valenta I, Gaemperli O, Siegrist PT, Tay FM, Burkhard N, Wyss CA, Kaufmann PA. Long-term prognostic value of 13N-ammonia myocardial perfusion positron emission tomography added value of coronary flow reserve. *J Am Coll Cardiol* 2009;**54**:150–156.
- Ziadi MC, Beanlands R, DeKemp R, Renaud J, RE T, Guo A, Williams K, Chow B, Ruddy TD, Hessian R, Garrard L, Davies RA, Etele J. Impaired MFR measured using Rb-82 predicts outcomes in patients with suspected ischemia. *Circulation* 2009;**120**:S320.
- Ziadi MC, Garrard L, Beanlands R, DeKemp R, Guo A, Williams K, Chow B, Ruddy TD, Renaud J, Hessian R, Davies RA, Etele J. Reduced MFR quantified Rb-82 is an independent prediction of 3-V CAD. *Circulation* 2009;**120**:S320–S321.
- Madar I, Ravert H, Dipaula A, Du Y, Dannals RF, Becker L. Assessment of severity of coronary artery stenosis in a canine model using the PET agent 18F-fluorobenzyl triphenyl phosphonium: comparison with 99mTc-tetrofosmin. *J Nucl Med* 2007;**48**:1021–1030.

38. Yu M, Guaraldi MT, Mistry M, Kagan M, McDonald JL, Drew K, Radeke H, Azure M, Purohit A, Casebier DS, Robinson SP. BMS-747158-02: a novel PET myocardial perfusion imaging agent. *J Nucl Cardiol* 2007;**14**:789–798.
39. Maddahi J, Schiepers C, Czernin J, Sparks R, Phelps M. First human study of BMS747158, a novel F-18 labeled tracer for myocardial perfusion imaging. *J Nucl Med* 2008;**49**:70P.
40. Tennant R, Wiggers C. Effect of coronary occlusion on myocardial contraction. *Am J Physiol* 1935;**112**:351–361.
41. Heyndrickx GR, Millard RW, McRitchie RJ, Maroko PR, Vatner SF. Regional myocardial functional and electrophysiological alterations after brief coronary artery occlusion in conscious dogs. *J Clin Invest* 1975;**56**:978–985.
42. Braunwald E, Kloner RA. The stunned myocardium: prolonged, postischemic ventricular dysfunction. *Circulation* 1982;**66**:1146–1149.
43. Ambrosio G, Betocchi S, Pace L, Losi MA, Perrone-Filardi P, Soricelli A, Piscione F, Taube J, Squame F, Salvatore M, Weiss JL, Chiariello M. Prolonged impairment of regional contractile function after resolution of exercise-induced angina. Evidence of myocardial stunning in patients with coronary artery disease. *Circulation* 1996;**94**:2455–2464.
44. Barnes E, Hall RJ, Dutka DP, Camici PG. Absolute blood flow and oxygen consumption in stunned myocardium in patients with coronary artery disease. *J Am Coll Cardiol* 2002;**39**:420–427.
45. Diamond GA, Forrester JS, deLuz PL, Wyatt HL, Swan HJ. Post-extrasystolic potentiation of ischemic myocardium by atrial stimulation. *Am Heart J* 1978;**95**:204–209.
46. Rahimtoola SH. A perspective on the three large multicenter randomized clinical trials of coronary bypass surgery for chronic stable angina. *Circulation* 1985;**72**:V123–V135.
47. Camici PG, Prasad SK, Rimoldi OE. Stunning, hibernation, and assessment of myocardial viability. *Circulation* 2008;**117**:103–114.
48. Schinkel AF, Bax JJ, Poldermans D, Elhendy A, Ferrari R, Rahimtoola SH. Hibernating myocardium: diagnosis and patient outcomes. *Curr Probl Cardiol* 2007;**32**:375–410.
49. Wijns W, Vatner SF, Camici PG. Hibernating myocardium. *N Engl J Med* 1998;**339**:173–181.
50. Depe C, Kim SJ, John AS, Huang Y, Rimoldi OE, Pepper JR, Dreyfus GD, Gausson V, Pennell DJ, Vatner DE, Camici PG, Vatner SF. Program of cell survival underlying human and experimental hibernating myocardium. *Circ Res* 2004;**95**:433–440.
51. Tillisch J, Brunken R, Marshall R, Schwaiger M, Mandelkern M, Phelps M, Schelbert H. Reversibility of cardiac wall-motion abnormalities predicted by positron tomography. *N Engl J Med* 1986;**314**:884–888.
52. Beanlands R, Ruddy T, de Kemp R, Iwanochko RM, Coates G, Freeman M, Nahmais C, Hendry P, Burns RJ, Lamy A, Mickleborough L, Kostuk W, Fallen E, Nichol G, PARR Investigators. Positron emission tomography and recovery following revascularization (PARR-1): the importance of scar and the development of a prediction rule for the degree of recovery of left ventricular function. *J Am Coll Cardiol* 2002;**40**:1735–1743.
53. Beanlands RS, Nichol G, Huszti E, Humen D, Racine N, Freeman M, Gulenchyn KY, Garrard L, de Kemp R, Guo A, Ruddy TD, Benard F, Lamy A, Iwanochko RM. F-18-fluorodeoxyglucose positron emission tomography imaging-assisted management of patients with severe left ventricular dysfunction and suspected coronary disease: a randomized, controlled trial (PARR-2). *J Am Coll Cardiol* 2007;**50**:2002–2012.
54. Bax JJ, Patton JA, Poldermans D, Elhendy A, Sandler MP. 18-Fluorodeoxyglucose imaging with positron emission tomography and single photon emission computed tomography: cardiac applications. *Semin Nucl Med* 2000;**30**:281–298.
55. Fallavollita JA, Luisi AJ Jr., Yun E, Dekemp RA, Cauty JM Jr. An abbreviated hyperinsulinemic-euglycemic clamp results in similar myocardial glucose utilization in both diabetic and non-diabetic patients with ischemic cardiomyopathy. *J Nucl Cardiol* 2010;**17**:637–645.
56. Sun KT, Yeatman L, Buxton D, Chen K, Johnson JA, Huang S-C, Kofoed KF, Weismueller S, Czernin J, Phelps ME, Schelbert HR. Simultaneous measurement of myocardial oxygen consumption and blood flow using [1-Carbon-11] acetate. *J Nucl Med* 1998;**39**:272–280.
57. Gropler R, Shelton ME, Herrero P, Walsh JF, Bergmann SR. Measurement of myocardial oxygen consumption using positron emission tomography and C-11 acetate: direct validation in human subjects. *Circulation* 1993;**88**:1–172.
58. He J, Ogden LG, Bazzano LA, Vupputuri S, Loria C, Whelton PK. Risk factors for congestive heart failure in US men and women: NHANES I epidemiologic follow-up study. *Arch Intern Med* 2001;**161**:996–1002.
59. Beanlands RS, Chow BJ, Dick A, Friedrich MG, Gulenchyn KY, Kiess M, Leong-Poi H, Miller RM, Nichol G, Freeman M, Bogaty P, Honos G, Hudon G, Wisenberg G, Van Berkom J, Williams K, Yoshinaga K, Graham J. CCS/CAR/CANM/CNCS/CanSCMR joint position statement on advanced noninvasive cardiac imaging using positron emission tomography, magnetic resonance imaging and multidetector computed tomographic angiography in the diagnosis and evaluation of ischemic heart disease—executive summary. *Can J Cardiol* 2007;**23**:107–119.
60. Beanlands R, Thorn S, DaSilva J, Ruddy T, Maddahi J. Myocardial viability. In: Wahl R, ed. *Principles and Practices of Positron Emission Tomography*. 2nd ed. Philadelphia: Lippincott Williams and Wilkins; 2008.
61. Dokainish H, Freidrich M, Ziadi MC, Beanlands R. Imaging in the patient with heart failure. In: Mann D, ed. *Heart Failure: A Companion to Braunwald's Heart Disease*. Philadelphia: Elsevier; 2010 (in press).
62. Tamaki N, Yonekura Y, Yamashita K, Saji H, Magata Y, Senda M, Konishi Y, Hirata K, Ban T, Konishi J. Positron emission tomography using fluorine-18-deoxyglucose in evaluation of coronary artery bypass grafting. *Am J Cardiol* 1989;**64**:860–865.
63. Vitale G, de Kemp R, Ruddy TD, Beanlands R. Myocardial glucose utilization and the optimization of F-18-FDG PET imaging in patients with NIDDM, CAD and LV dysfunction. *J Nucl Med* 2001;**42**:1730–1736.
64. vom Dahl J, Eitzman DT, Al-Aouar ZR, Kanter HL, Hicks RJ, Deeb GM, Kirsch MM, Schwaiger M. Relation of regional function, perfusion, and metabolism in patients with advanced coronary artery disease undergoing surgical revascularization. *Circulation* 1994;**90**:2356–2365.
65. Di Carli MF, Davidson M, Little R, Khanna S, Mody FV, Brunken RC, Czernin J, Rokhsar S, Stevenson LW, Laks H, Hawkins R, Schelbert HR, Phelps ME, Maddahi J. Value of metabolic imaging with positron emission tomography for evaluating prognosis in patients with coronary artery disease and left ventricular dysfunction. *Am J Cardiol* 1994;**73**:527–533.
66. D'Egidio G, Nichol G, Williams K, Guo A, Garrard L, de Kemp R, Ruddy T, DaSilva J, Humen D, Gulenchyn K, Freeman M, Racine N, Benard F, Hendry P, Beanlands R. Identification of high-risk patients with increasing ischemic cardiomyopathy. *JACC Cardiovasc Imaging* 2009;**2**:1060–1068.
67. Inaba Y, Chen JA, Bergmann SR. Quantity of viable myocardium required to improve survival with revascularization in patients with ischemic cardiomyopathy: a meta-analysis. *J Nucl Cardiol* 2010;**17**:646–654.
68. Medical Advisory Secretariat. Positron emission tomography (PET) for the assessment of myocardial viability: an evidence-based analysis. [http://www.health.gov.on.ca/english/providers/program/ohctac/tech/draft\\_comment/rev\\_cardiacmyo\\_pet\\_20100429.pdf](http://www.health.gov.on.ca/english/providers/program/ohctac/tech/draft_comment/rev_cardiacmyo_pet_20100429.pdf) (6 July 2010).
69. Thompson K, Saab G, Birnie D, Chow BJ, Ukkonen H, Ananthasubramanian K, Dekemp RA, Garrard L, Ruddy TD, Dasilva JN, Beanlands RS. Is septal glucose metabolism altered in patients with left bundle branch block and ischemic cardiomyopathy? *J Nucl Med* 2006;**47**:1763–1768.
70. Inoue N, Takahashi N, Ishikawa T, Sumita S, Kobayashi T, Matsushita K, Matsumoto K, Taima M, Shimura M, Uchino K, Kimura K, Inoue T, Umemura S. Reverse perfusion-metabolism mismatch predicts good prognosis in patients undergoing cardiac resynchronization therapy: a pilot study. *Circ J* 2007;**71**:126–131.
71. Birnie D, DeKemp RA, Ruddy TD, Tang AS, Guo A, Williams K, Wassenar R, Lalonde M, Beanlands RS. Effect of lateral wall scar on reverse remodeling with cardiac resynchronization therapy. *Heart Rhythm* 2009;**6**:1721–1726.
72. Ypenburg C, Schalijs MJ, Bleeker GB, Steendijk P, Boersma E, Dibbets-Schneider P, Stokkel MP, van der Wall EE, Bax JJ. Extent of viability to predict response to cardiac resynchronization therapy in ischemic heart failure patients. *J Nucl Med* 2006;**47**:1565–1570.
73. DeFronzo R, Tobin J, Andres R. Glucose clamp technique: a method for quantifying insulin secretion and resistance. *Am J Physiol* 1979;**273**:E214–E223.
74. Paternostro G, Camici PG, Lammerstma AA, Marinho N, Baliga RR, Kooner JS, Radda GK, Ferrannini E. Cardiac and skeletal muscle insulin resistance in patients with coronary heart disease. A study with positron emission tomography. *J Clin Invest* 1996;**98**:2094–2099.
75. Marinho NVS, Keogh BE, Costa DC, Lannerstma AA, Ell PJ, Camici PG. Pathophysiology of chronic left ventricular dysfunction: new insights from the measurement of absolute myocardial blood flow and glucose utilization. *Circulation* 1996;**93**:737–744.
76. Fath-Ordoubadi F, Beatt KJ, Spyrou N, Camici PG. Efficacy of coronary angioplasty for the treatment of hibernating myocardium. *Heart* 1999;**82**:210–216.
77. Lautamaki R, Airaksinen KE, Seppanen M, Toikka J, Luotolahti M, Ball E, Borra R, Harkonen R, Iozzo P, Stewart M, Knuuti J, Nuutila P. Rosiglitazone improves myocardial glucose uptake in patients with type 2 diabetes and coronary artery disease: a 16-week randomized, double-blind, placebo-controlled study. *Diabetes* 2005;**54**:2787–2794.
78. Knuuti MJ, Saraste M, Nuutila P, Härkönen R, Wegelius U, Haapanen A, Bergman J, Haaparanta M, Savunen T, Voipio-Pulkki LM. Myocardial viability: fluorine-18-deoxyglucose positron emission tomography in prediction of wall motion recovery after revascularization. *Am Heart J* 1994;**127**:785–796.

79. Marwick T, MacIntyre WJ, Lafont A, Nemecek JJ, Salcedo EE. Metabolic responses of hibernating and infarcted myocardium to revascularization. A follow-up study of regional perfusion, function, and metabolism. *Circulation* 1992;**85**:1347–1353.
80. Start RH, Bax JJ, van Veldhuisen DJ, van der Wall EE, Irwan R, Sluiter WJ, Dierckx RA, de Boer J, Jager PL. Prediction of functional recovery after revascularization in patients with chronic ischaemic left ventricular dysfunction: head-to-head comparison between <sup>99m</sup>Tc-sestamibi/<sup>18</sup>F-FDG DISA SPECT and <sup>13</sup>N-ammonia/<sup>18</sup>F-FDG PET. *Eur J Nucl Med Mol Imaging* 2006;**33**:716–723.
81. Start RH, Bax JJ, van Veldhuisen DJ, van der Wall EE, Dierckx RA, de Boer J, Jager PL. Prediction of functional recovery after revascularization in patients with coronary artery disease and left ventricular dysfunction by gated FDG-PET. *J Nucl Cardiol* 2006;**13**:210–219.
82. Siebelink H-M, Blanksma PK, Crijns H, Bax JJ, Van Boven AJ, Kingma T, Piers D, Pruijm J, Jager P, Vaalburg W, van der Wall EE. No difference in cardiac event-free survival between positron emission tomography-guided and single-photon emission computed tomography-guided management. *J Am Coll Cardiol* 2001;**37**:81–88.
83. Eitzman D, Al-Aouar Z, Kanter HL, vom Dahl J, Kirsch M, Deeb GM, Schwaiger M. Clinical outcome of patients with advanced coronary artery disease after viability studies with positron emission tomography. *J Am Coll Cardiol* 1992;**20**:559–565.
84. Lee KS, Marwick TH, Cook SA, Go RT, Fix JS, James KB, Sapp SK, MacIntyre WJ, Thomas JD. Prognosis of patients with left ventricular dysfunction, with and without viable myocardium after myocardial infarction: Relative efficacy of medical therapy and revascularization. *Circulation* 1995;**90**:2687–2694.
85. Allman KC, Shaw LJ, Hachamovitch R, Udelson JE. Myocardial viability testing and impact of revascularization on prognosis in patients with coronary artery disease and left ventricular dysfunction: a meta-analysis. *J Am Coll Cardiol* 2002;**39**:1151–1158.
86. Desideri A, Cortigiani L, Christen AI, Coscarelli S, Gregori D, Zanco P, Komorovsky R, Bax JJ. The extent of perfusion-F18-fluorodeoxyglucose positron emission tomography mismatch determines mortality in medically treated patients with chronic ischemic left ventricular dysfunction. *J Am Coll Cardiol* 2005;**46**:1264–1269.
87. Pitt M, Dutka D, Pagano D, Camici P, Bonser R. The natural history of myocardium awaiting revascularisation in patients with impaired left ventricular function. *Eur Heart J* 2004;**25**:500–507.
88. Beanlands RS, Hendry P, Masters R, de Kemp RA, Woodend K, Ruddy TD. Delay in revascularization is associated with increased mortality rate in patients with severe LV dysfunction and viable myocardium on fluorine-18-fluorodeoxyglucose positron emission tomography imaging. *Circulation* 1998;**98**:II-51–II-56.
89. Lee KS, Marwick TH, Cook SA, Go RT, Fix JS, James KB, Sapp SK, MacIntyre WJ, Thomas JD. Prognosis of patients with left ventricular dysfunction, with and without viable myocardium after myocardial infarction. Relative efficacy of medical therapy and revascularization. *Circulation* 1994;**90**:2687–2694.
90. Steel K, Broderick R, Gandla V, Larose E, Resnic F, Jerosch-Herold M, Brown KA, Kwong RY. Complementary prognostic values of stress myocardial perfusion and late gadolinium enhancement imaging by cardiac magnetic resonance in patients with known or suspected coronary artery disease. *Circulation* 2009;**120**:1390–1400.
91. McMurray JJ. Clinical practice. Systolic heart failure. *N Engl J Med* 2010;**362**:228–238.
92. Dickstein K, Cohen-Solal A, Filippatos G, McMurray JJ, Ponikowski P, Poole-Wilson PA, Stromberg A, van Veldhuisen DJ, Atar D, Hoes AW, Keren A, Mebazaa A, Nieminen M, Priori SG, Swedberg K, Vahanian A, Camm J, De Caterina R, Dean V, Funck-Brentano C, Hellemans I, Kristensen SD, McGregor K, Sechtem U, Silber S, Tendera M, Widimsky P, Zamorano JL. ESC Guidelines for the diagnosis and treatment of acute and chronic heart failure 2008: the Task Force for the Diagnosis and Treatment of Acute and Chronic Heart Failure 2008 of the European Society of Cardiology. Developed in collaboration with the Heart Failure Association of the ESC (HFA) and endorsed by the European Society of Intensive Care Medicine (ESICM). *Eur Heart J* 2008;**29**:2388–2442.
93. Velazquez EJ, Lee KL, O'Connor CM, Oh JK, Bonow RO, Pohost GM, Feldman AM, Mark DB, Panza JA, Sopko G, Rouleau JL, Jones RH. The rationale and design of the Surgical Treatment for Ischemic Heart Failure (STICH) trial. *J Thorac Cardiovasc Surg* 2007;**134**:1540–1547.
94. Jones RH, Velazquez EJ, Michler RE, Sopko G, Oh JK, O'Connor CM, Hill JA, Menicanti L, Sadowski Z, Desvigne-Nickens P, Rouleau JL, Lee KL. Coronary bypass surgery with or without surgical ventricular reconstruction. *N Engl J Med* 2009;**360**:1705–1717.
95. Serruys PW, Morice MC, Kappetein AP, Colombo A, Holmes DR, Mack MJ, Stahle E, Feldman TE, van den Brand M, Bass EJ, Van Dyck N, Leadley K, Dawkins KD, Mohr FW. Percutaneous coronary intervention versus coronary-artery bypass grafting for severe coronary artery disease. *N Engl J Med* 2009;**360**:961–972.
96. Pagano D, Fath-Ordoubadi F, Beatt KJ, Townend JN, Bonser RS, Camici PG. Effects of coronary revascularisation on myocardial blood flow and coronary vasodilator reserve in hibernating myocardium. *Heart* 2001;**85**:208–212.
97. Camici PG, Dutka DP. Repetitive stunning, hibernation, and heart failure: contribution of PET to establishing a link. *Am J Physiol Heart Circ Physiol* 2001;**280**:H929–H936.
98. Gropler RJ, Beanlands RS, Dilsizian V, Lewandowski ED, Villanueva FS, Ziadi MC. Imaging myocardial metabolic remodeling. *J Nucl Med* 2010;**51**:1S–14.